Relativistic kinetic theory of pitch angle scattering, slowing down, and energy deposition in a plasma

J. Robiche and J. M. Rax*
Laboratoire de Physique et Technologie des Plasmas, Ecole Polytechnique, 91128 Palaiseau Cedex, France
(Received 15 December 2003; published 8 October 2004)

The collisional dynamics of a relativistic electron population in a Lorentzian plasma are investigated and analyzed within the framework of kinetic theory. The relativistic Fokker-Planck equation describing both slowing down and pitch angle scattering is derived, analyzed, and solved. The analytical Green function is used to express the electron range, the range straggling, and the mean radial dispersion as a function of the plasma parameters. Compared to standard slowing down theories, the inclusion of the pitch angle scattering without any Gaussian approximation appears to be essential to calculate these quantities.

DOI: 10.1103/PhysRevE.70.046405 PACS number(s): 52.20.Fs, 52.50.Gj, 52.25.Tx, 52.25.Dg

I. INTRODUCTION

Fast electron energy deposition is a long-standing problem which has received a lot of attention within various contexts [1–4]. In plasmas, several models have been put forward to address and solve this problem. Both pure slowing down theory, where pitch angle scattering is ignored, or improved slowing down based on a Gaussian approximation [5] of pitch angle dynamic have been used in the past. Surprisingly, no attempt to solve this problem with the exact solution of the relativistic electron kinetic equation has been reported in the literature. In this paper, we show that this relativistic kinetic equation can be solved analytically and that the characteristics of the electron energy deposition volume can be expressed as a function of the initial energy and the plasma parameters.

Recently, slowing down calculations have been reevaluated for laser-plasma studies [6]. The development of a compact, high-power, subpicosecond laser based on chirped pulse amplification has opened a new field of laser plasma interaction. In the terawatt to petawatt regime, the electron quiver velocity becomes relativistic and a whole set of new relativistic nonlinear processes appears. At the beginning of the decade, those processes relevant to the design of advanced accelerators or advanced light sources, such as harmonic generation [7,8], wake generation [9], and magnetic field generation [10], were widely investigated. Besides these fundamental studies on underdense targets, the proposal to use relativistic nonlinearities to generate a jet of relativistic electrons in order to ignite a thermonuclear target has received a lot of attention [6]. Within the framework of this program, two issues are to be addressed: (i) the understanding of the mechanism producing this burst of relativistic electrons in order to optimize the production step; (ii) the precise evaluation of the hot spot size in order to access the potential for ignition. Moreover, these relativistic electron bursts have been identified as a free energy source for x-ray generation through bremsstrahlung in a dense target [11]; again, in order to optimize such a source, a precise evaluation of the electron dynamics is required and the issue of pitch angle scattering becomes of prime importance as this later process is the ultimate source of x-ray radiation.

This paper addresses the issue of the relativistic collisional dynamics of energetic electrons. Kinetic theory provides the right framework to address this problem as the electron-ion interaction cannot be reduced to a slowing down and is intrinsically a random process.

When a relativistic electron interacts with a plasma, two types of interaction determine the dynamics: the electron-electron interaction and the electron-ion interaction. Although the first can be treated as a deterministic slowing down, the second gives rises to pitch angle scattering and determines the size of the energy deposition volume. The fact that pitch angle scattering is essential to calculate the heated volume size can be understood as follows. The slowing down time scale of a relativistic electron is $\tau = [4\pi c n_e r_e^2 \ln \Lambda_{ee}]^{-1}$, where we use the following notation: n_e is the electron density, r_e is the classical electron radius, and c is the velocity of light. The time scale for pitch angle scattering is $2\tau \ln \Lambda_{ee}/Z \ln \Lambda_{ei} = 2\tau/Z\Lambda$, where Z is the ion charge state, $\log \Lambda_{es}$ is the Coulomb logarithm for relativistic electron colliding with background species ($s=e,i$), and $\Lambda = \ln \Lambda_{ei}/\ln \Lambda_{ee} \sim 1$ is the Coulomb logarithm ratio. This scaling means that the cumulative Coulomb small-angle scattering will turn the electron trajectory by an average angle of $\pi/2$ on a time scale of the order of the slowing down time.

We will address this issue of simultaneous slowing down and pitch angle scattering without the usual Gaussian approximation [5]; rather than this approximation, we will consider the solution of the full relativistic kinetic equation. The Green function of the relativistic kinetic operator provides the right framework to calculate both the transverse and longitudinal size of the heated volume and has already been successfully used for current drive and the turbulence problems [12,13]. It turns out that the key parameters describing energy deposition can be exactly evaluated in compact analytical form so that the scaling with respect to the various beam and plasma conditions can be explicitly displayed and analyzed.

This paper is organized as follows. In the next section, we set up the various model assumptions. In Sec. III, we recall

*Electronic address: rax@lptp.polytechnique.fr

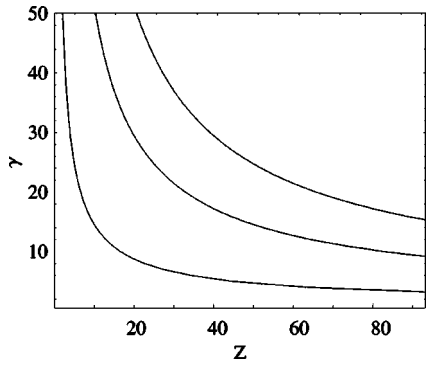

FIG. 1. Ratio of radiative to collisional energy loss in the (Z,γ) plane. Lower, intermediate, and upper curves correspond, respectively, to radiative loss equal to 10%, 50%, and 100% of the collisional loss.

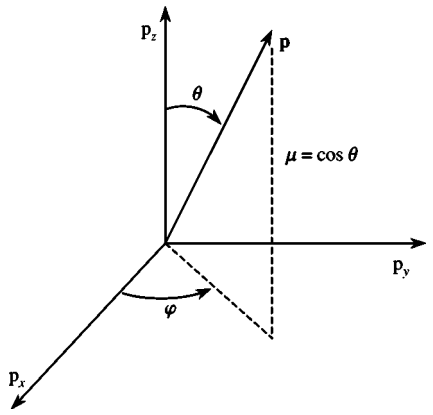

FIG. 2. Definition of the set of spherical momentum coordinates (p,θ,ϕ).

and discuss the standard form of the kinetic operator describing relativistic electron dynamics in a cold plasma. We use the Belieav and Budker relativistic extension of the Landau collision kernel in order to set up the relativistic kinetic equation. Then, in Sec. IV, we solve this equation with the use of the Green-function method. Sections V and VI address the issue of the explicit analytical evaluation of the mean penetration depth, the radial dispersion, and the longitudinal spreading of the electron beam. In the final section, we summarize our main findings.

Throughout this paper, in order to simplify this study, we will use the relativistic slowing down time τ as the unit of time and $m_e c$ as the unit of momentum. Thus, the unit of length is $\lambda = c \times \tau$,

$$\left[\frac{\lambda}{\mathrm{cm}}\right] = \frac{1}{\ln \Lambda_{ee}}\left[\frac{10^{30}\ \mathrm{m}^{-3}}{n_e}\right]. \tag{1}$$

The relativistic momentum is denoted $\mathbf{p} = \gamma \mathbf{v}$ and the relativistic energy is $\gamma = \sqrt{1+\mathbf{p}^2}$.

II. MODEL ASSUMPTIONS

An electron interacting with a plasma loses energy and momentum through two main channels: (i) collisions and (ii) radiation. Collisional energy loss leads to a *continuous slowing down* while bremsstrahlung causes large and sudden energy losses. Over the energy range considered in this paper, the contribution due to bremsstrahlung remains negligible so that we will restrict our study to the case where collisional energy loss is the dominant process. The ratio of the radiative energy loss $|d\gamma/dx|_{\mathrm{rad}}$ (see Ref. [11]) to the collisional energy loss $|d\gamma/dx|_{\mathrm{col}}$ is depicted in Fig. 1 as a line of constant contour in the (Z,γ) plane. Clearly, for electron energy below a few MeV, radiative losses contribute only for about a few percent of the total loss.

Besides this classical assumption, a second assumption concerns the electric and magnetic fields. Self-generated magnetic fields reduce the radial spread and increase the penetration, and self-generated electric fields decelerate the electrons and decrease the penetration. Although the Green-function method offers an efficient framework to develop a perturbative analysis, these issues are not addressed here; in this first paper, we have neglected collective field effects on the grounds that fast charge and current neutralization take place in a high conductivity medium.

Then, provided the beam density is small compared to the background plasma density, we can neglect interaction between electrons of the beam so that the electron jet-plasma interaction reduces to that of a linear superposition of isolated fast electrons.

III. LANDAU AND BELIAEV-BUDKER KINETIC OPERATORS

In order to study the interaction between a relativistic electron and a background plasma described by F_e and F_i, the electron and ion plasma distribution function, we have to set up and solve the kinetic equation for the relativistic momentum electron distribution function $f(\mathbf{p},t)$, including both collisional drag and angular scattering. We describe the electron-electron and electron-ion interactions by two collisional operators $\mathbf{C}_{ee}$ and $\mathbf{C}_{ei}$ so that the kinetic equation governing the evolution of the electron momentum distribution function f reads

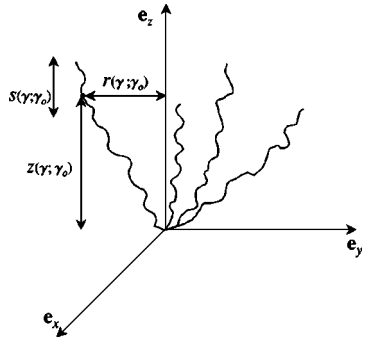

FIG. 3. Sketch of a generic electron trajectory undergoing small-angle collision scattering off background plasma and definition of the three characteristic lengths: $\langle z \rangle$ is the mean distance traveled by an electron along $\mathbf{e}_z$, $\langle r^2 \rangle^{1/2}$ is the mean radius, and s is the straggling factor defined in the text.

$$\partial f/\partial t = \mathbf{C}_{ei}(f,F_i) + \mathbf{C}_{ee}(f,F_e). \tag{2}$$

As far as we consider fast electrons (few MeV) interacting with a thermal background plasma, the thermal velocity of the plasma species can be neglected. Therefore, it is a reasonable approximation to represent the background distribution by two "cold" distributions

$$F_s(\mathbf{p}_s) = n_s \frac{\delta(p_s)}{4\pi p_s^2}, \tag{3}$$

where $s=e,i$ denotes the background species and $p_s=|\mathbf{p}_s|$; F_s is normalized to species s and density n_s,

$$\int F_s(\mathbf{p}) d^3\mathbf{p} = n_s. \tag{4}$$

Furthermore, quasineutrality implies $n=n_e=Z\,n_i$. These collision operators can be expressed in terms of a collision kernel $\mathbf{U}(\mathbf{p},\mathbf{p}')$, which is merely the Fourier transform of the screened Coulomb potential [14,15],

$$\mathbf{C}_{ab}(f_a,f_b) = \frac{q_a^2 q_b^2 \ln\Lambda_{ab}}{8\pi\varepsilon_0^2} \frac{\partial}{\partial \mathbf{p}} \cdot \int \mathbf{U}(\mathbf{p},\mathbf{p}') \times \left[f_b(\mathbf{p}') \frac{\partial f_a}{\partial \mathbf{p}} - f_a(\mathbf{p}) \frac{\partial f_b}{\partial \mathbf{p}} \right] d\mathbf{p}', \tag{5}$$

where q_s is the charge of the species s, $\ln\Lambda_{ab}$ is the Coulomb logarithm associated with the population a interacting with species b, and ε_0 is the permittivity of free space. This classical *Landau* form of this kernel is given by [16]

$$\mathbf{U}(\mathbf{p},\mathbf{p}') = \mathbf{I} - \frac{(\mathbf{p}-\mathbf{p}')(\mathbf{p}-\mathbf{p}')}{(\mathbf{p}-\mathbf{p}')^2}, \tag{6}$$

where $\mathbf{I}$ is the unit tensor. Beliaev and Budker have developed the relativistic form of this classical kernel. They obtained the following expression, which is a Lorentz invariant [12,15,17,18]:

$$\mathbf{U}(\mathbf{p},\mathbf{p}') = \frac{(\gamma\gamma' - \mathbf{p}\cdot\mathbf{p}')^2 \{[(\gamma\gamma' - \mathbf{p}\cdot\mathbf{p}')^2 - 1]\mathbf{I} - \mathbf{p}\mathbf{p} - \mathbf{p}'\mathbf{p}' + (\gamma\gamma' - \mathbf{p}\cdot\mathbf{p}')(\mathbf{p}\mathbf{p}' + \mathbf{p}'\mathbf{p})\}}{\gamma\gamma'[(\gamma\gamma' - \mathbf{p}\cdot\mathbf{p}')^2 - 1]^{3/2}}. \tag{7}$$

Substituting this relativistic kernel Eq. (7) into the collision integrals $\mathbf{C}_{ee}$ and $\mathbf{C}_{ei}$ [Eq. (5)] and using Eq. (3) for the background distribution function, we obtain the Fokker-Planck form of the normalized (to τ) collision operator $\mathbf{C}_{ee}+\mathbf{C}_{ei}$, the Beliaev-Budker relativistic operator [12,18],

$$\mathbf{C}_{ee}(f,F)_e + \mathbf{C}_{ei}(f,F)_i = -\frac{1}{p^2}\frac{\partial}{\partial p}\gamma^2 f - \frac{1+Z\Lambda}{2}\frac{\gamma}{p^3}\left[\frac{\partial}{\partial\mu}(1-\mu^2)\frac{\partial}{\partial\mu} + \frac{1}{1-\mu^2}\frac{\partial^2}{\partial\varphi^2}\right] f, \tag{8}$$

where we have performed the integrations using spherical coordinates in momentum space (p,θ,φ), where $\mathbf{p}=p_x\mathbf{e}_x+p_y\mathbf{e}_y+p_z\mathbf{e}_z$, $p_z=p\mu$, $p_x=p\sqrt{1-\mu^2}\cos\varphi$, $p_y=p\sqrt{1-\mu^2}\sin\varphi$, and $\mu=\cos\theta$ (Fig. 2); $(\mathbf{e}_x,\mathbf{e}_y,\mathbf{e}_z)$ is a Cartesian basis. We have also introduced the Coulomb logarithm ratio $\Lambda=\ln\Lambda_{ee}/\ln\Lambda_{ei}$. For moderately relativistic electrons (up to a few tens of MeV) and for low values of Z, this ratio is close to unity $\Lambda\sim 1$ [19].

The first part on the right-hand side of Eq. (8) describes the effect of collisional drag due to electron-electron collisions while the second part describes pitch angle scattering due to both electron-electron and electron-ion collisions. Collisional drag leads to deterministic slowing down and pitch angle scattering to diffusion in momentum space.

IV. GREEN FUNCTION OF THE BELIAEV-BUDKER OPERATOR

We now consider the following initial value problem: a relativistic electron is embedded in a plasma with a momentum $\mathbf{p}_0$ and a position $\mathbf{r}_0=(0,0,0)$ at time $t_0=0$. This corresponds to an initial distribution function represented by a shifted Dirac function $f(\mathbf{p},t_0)=\delta(\mathbf{p}-\mathbf{p}_0)$. The evolution of $f(\mathbf{p},t)(t>t_0)$ is just the Green function of the Beliaev-Budker operator and we have $f(\mathbf{p},t)=G(\mathbf{p},\mathbf{p}_0,t,t_0)$, where G is the solution of

$$\frac{\partial G}{\partial t} - \frac{1}{p^2}\frac{\partial}{\partial p}\gamma^2 G - \frac{1+Z\Lambda}{2}\frac{\gamma}{p^3}\left[\frac{\partial}{\partial\mu}(1-\mu^2)\frac{\partial}{\partial\mu} + \frac{1}{1-\mu^2}\frac{\partial^2}{\partial\varphi^2}\right] G = \frac{\delta(p-p_0)}{p^2}\delta(\mu-\mu_0)\delta(\varphi-\varphi_0)\delta(t-t_0). \tag{9}$$

(p_0,μ_0,φ_0) are the spherical initial momentum coordinates at time $t_0=0$. Despite this apparent complexity, G can be explicitly calculated [12,20]. It is convenient to expand the solution of Eq. (9) on the spherical harmonics basis since they are the eigenfunctions of the angular part of the collision operator [16]. With this spherical harmonic expansion, the solution of Eq. (9) can be written as

$$G = \frac{\delta(\arctan(p) - p - \arctan(p_0) + p_0 - (t - t_0))}{\gamma^2} H(t - t_0) \sum_{l=0}^{l=+\infty} \sum_{m=-l}^{m=+l} Y_l^m(\mu, \varphi) Y_l^{m*}(\mu_0, \varphi_0) \left[\frac{p(\gamma_0 + 1)}{p_0(\gamma + 1)} \right]^{[l(l+1)(Z\Lambda+1)/2]}, \quad (10)$$

where the function Y_l^m is the spherical harmonic [21] and H is the Heaviside function. It is important to stress that Eq. (10) contains the complete collisional history of a relativistic electron beam moving in a background plasma and that this description does not require any Gaussian-type approximation for pitch angle scattering correlation. Clearly, the pitch angle diffusion is not described by a Gaussian kernel and the algebraic behavior of the μ dynamic invalidates the exponential dynamic assumed in such a Gaussian-type approximation. In this latter approximation, the argument of the exponential is the square of the angle so that large-angle deviation resulting from cumulative small-angle scattering cannot be described; moreover, the tail of the exponential decreases faster than any power of this argument, although the behavior of the tail of the fully kinetic is clearly algebraic.

This Green function $G(\mathbf{p}, \mathbf{p}_0, t, t_0)$ has a straightforward physical interpretation in term of *transition probability*: an electron starting at time t_0 with momentum $\mathbf{p}_0$ will be found with the probability $G(\mathbf{p}, \mathbf{p}_0, t, t_0) d\mathbf{p}$ at later time t in the momentum volume element $d\mathbf{p}$ centered around $\mathbf{p}$. Note that this Green function fulfills the Chapman-Kolmogorov identity

$$G(\mathbf{p}, \mathbf{p}_0, t, t_0) = \int d\mathbf{p}' G(\mathbf{p}, \mathbf{p}', t, t') G(\mathbf{p}', \mathbf{p}_0, t', t_0), \quad (11)$$

whose meaning is the following: the transition probability from $\mathbf{p}_0$ at t_0 to $\mathbf{p}$ at t can be obtained by summing over all possible intermediate states $\mathbf{p}'$ at time t' the product of the probabilities of transition $(\mathbf{p}_0, t_0) \rightarrow (\mathbf{p}', t')$ and $(\mathbf{p}', t') \rightarrow (\mathbf{p}, t)$.

The δ function appearing in the Green function Eq. (10) is a consequence of the deterministic slowing down of the fast electron due to collision with background cold electrons. The function inside the δ symbol gives an implicit form for $p(t)$,

$$\arctan(p) - p - \arctan(p_0) + p_0 - (t - t_0) = 0. \quad (12)$$

From this relation between momentum and time, we can easily obtain the slowing down time $t_s - t_0$ by setting $p = 0$ at $t = t_s$,

$$t_s = p_0 - \arctan p_0, \quad (13)$$

where t_s is normalized to τ. From the implicit relation between p and t, we obtain the following expression for the collisional energy-loss rate $d\gamma/dt = -\gamma/p$. G is a *transition probability* and is also a *propagator* so that it can be used to express the evolution of any $f(\mathbf{p}, t)$,

$$f(\mathbf{p}, t) = \int d\mathbf{p}_0 f(\mathbf{p}_0, t_0) G(\mathbf{p}, \mathbf{p}_0, t, t_0). \quad (14)$$

In the following, we are concerned about the propagation of a single relativistic electron, as the generalization to an arbitrary initial distribution function $f(\mathbf{p}_0)$ can be easily achieved through linear combination in Eq. (14).

V. ENERGY DEPOSITION PROFILE AND MEAN PENETRATION DEPTH

We have depicted a generic electron trajectory in Fig. 3, where $(\mathbf{e}_x, \mathbf{e}_y, \mathbf{e}_z)$ is a Cartesian basis. Kinetic energy is delivered to the target plasma all along the path followed by a fast electron. Hence, to evaluate the size of the plasma volume heated by the relativistic electron, we have to calculate not only the penetration depth but also the radial dispersion of the electrons and the longitudinal spreading.

Thus, to quantify the size of the heated volume, we define three characteristic lengths [2,22]: (i) the *mean penetration depth* $\langle z \rangle$, (ii) the longitudinal dispersion or *straggling factor* $s = \sqrt{\langle z \rangle^2 - \langle z^2 \rangle}$ defining the statistical spreading of a set of electrons with the same initial condition, and (iii) the *mean*

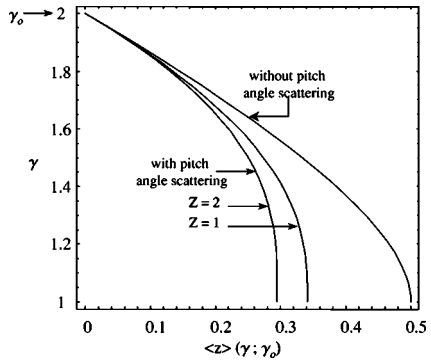

FIG. 4. Energy deposition profile of a 1 MeV electron for $Z = 1$ and $Z = 2$. Also plotted is the case where pitch angle scattering has been ignored. Length is normalized to λ [see Eq. (1)].

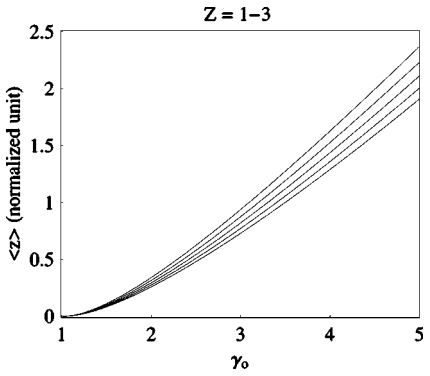

FIG. 5. Slowing down length for $Z = 1$, 3/2, 2, 5/2, and 3. The upper curve is for $Z = 1$. Length is normalized to λ [see Eq. (1)].

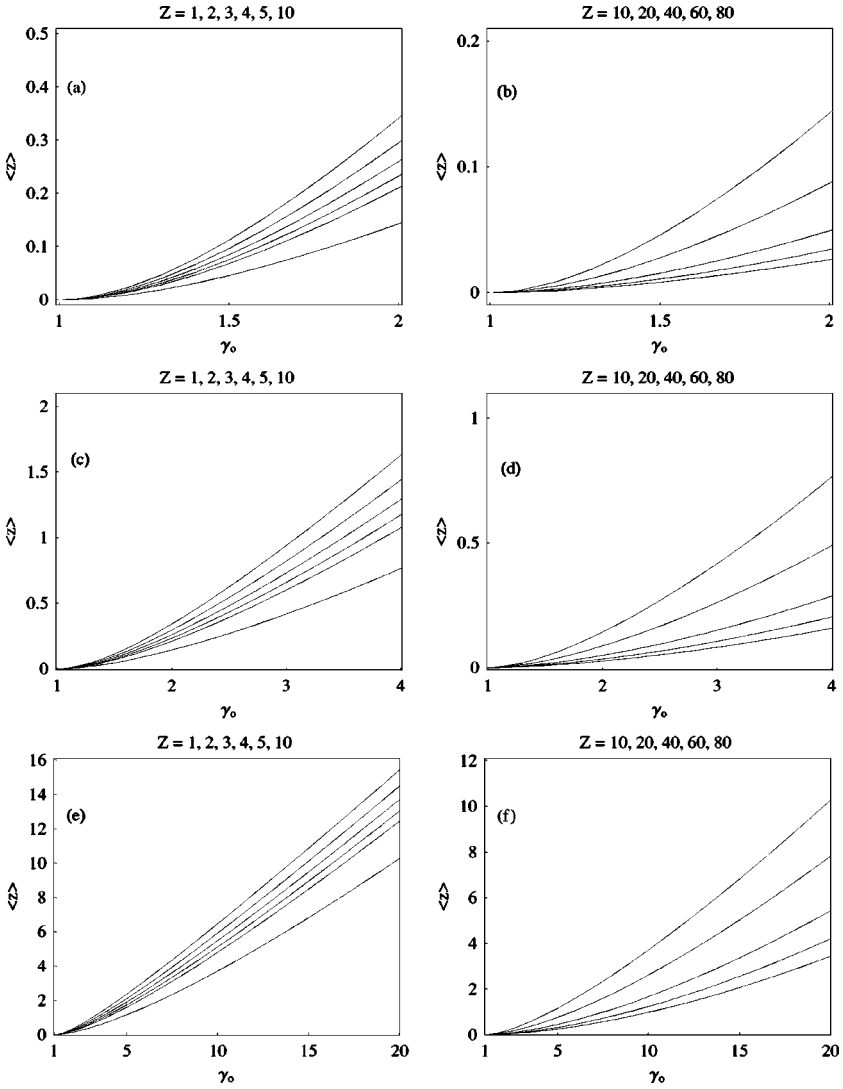

FIG. 6. Slowing down length vs initial energy γ_0. (a), (c), and (e) are for $Z=1$, 2, 3, 4, 5, and 10 and for γ_0 ranging, respectively, from 1 to 2, 1 to 4, and 1 to 20. (b), (d), and (f) are for $Z=10$, 20, 40, 60, and 80. Length is normalized to λ [see Eq. (1)].

radial size of the heated volume $\sqrt{\langle r^2\rangle}$. Here, the brackets $\langle\rangle$ stand for an average over the various realizations of the collisional noise. An explicit procedure for this average is defined below.

A. Mean penetration depth

We will consider the mean longitudinal position as a function of the energy. In order to determine this quantity, we write down the *stochastic Langevin equation* of motion averaged over the various realizations of the collisional noise,

$$\left\langle \frac{dz}{dt} \right\rangle = \frac{d\langle z\rangle}{dt} = \left\langle \frac{p}{\gamma}\cos\ \theta \right\rangle. \tag{15}$$

The velocity $v_z = p\cos\theta/\gamma$ is a *random* function of time because of pitch angle scattering. Then, based on the equivalence between a *Fokker-Planck* equation and a *Langevin* equation [12], the previous statistical average over the realizations of the collisional noise can be performed through the following substitution [7]:

$$\langle g(\mathbf{p})\rangle = \int d\mathbf{p}\ g(\mathbf{p}) G(\mathbf{p},\mathbf{p}_0,t,t_0), \tag{16}$$

where $g(\mathbf{p})$ is any function of the stochastic variable $\mathbf{p}$. As we have expanded G over the set of the spherical harmonic functions Y_l^m, we express the longitudinal velocity over the same basis,

$$\frac{dz}{dt} = \frac{p}{\gamma}\cos\ \theta = \sqrt{\frac{4\pi}{3}}\frac{p}{\gamma} Y_1^0(\mu,\varphi). \tag{17}$$

We insert Eq. (17) into Eq. (15) and perform the average (16). We obtain the following expression:

$$\frac{d\langle z\rangle}{dt} = \int d\mathbf{p}\ \sqrt{\frac{4\pi}{3}}\frac{p}{\gamma} Y_1^0(\mu,\varphi) G(\mathbf{p},\mathbf{p}_0,t,t_0). \tag{18}$$

The integration over the momentum volume element $d\mathbf{p} = p^2 d\mu\ d\phi$ can be achieved with the help of the orthogonal properties of the spherical harmonics and the Dirac identity $\delta(f(x)) = \Sigma_i\ \delta(x-x_i)/|f'(x)|_{x=x_i}$. Thus

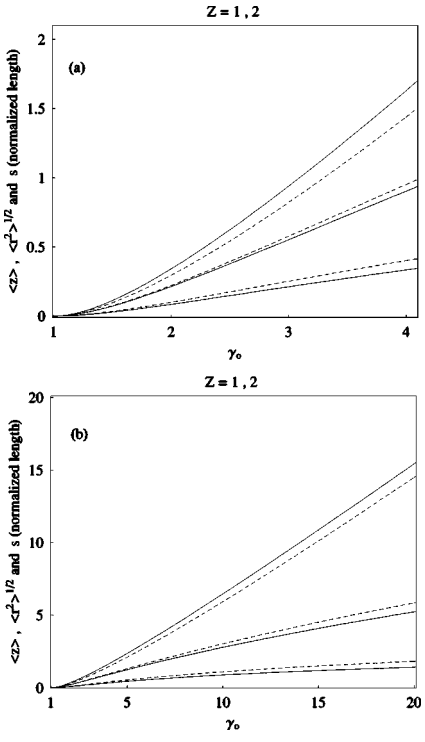

FIG. 7. Slowing down length $\langle z\rangle(1;\gamma_0)$, mean radius to $\langle r^2\rangle^{1/2}$, and straggling length s vs initial energy γ_0 for $Z=1$ (solid lines) and $Z=2$ (dotted lines). (a) Energy γ_0 range from 1 to 4, (b) energy γ_0 range from 1 to 20. All lengths are normalized to λ; see Eq. (1). Upper curves correspond to $\langle z\rangle$, intermediate curves to $\langle r^2\rangle^{1/2}$, and lower curves to s.

$$\delta(\arctan(p)-p-\arctan(p_0)+p_0-(t-t_0)) = \frac{\gamma^2(t)}{p^2(t)}\delta(p-p(p_0,t_0,t)), \tag{19}$$

where $p(p_0,t_0,t)$ is the zero for p of the function in the δ symbol. The velocity along $\mathbf{e}_z$ is finally given by

$$\frac{d\langle z\rangle}{dt} = -\frac{p(t)}{\gamma(t)}\left\{\frac{[\gamma(t)-1](\gamma_0+1)}{[\gamma(t)+1](\gamma_0-1)}\right\}^{(Z\Lambda+1)/2}, \tag{20}$$

where $p(t)$ $[\gamma(t)]$ must be understood as $p(p_0,t_0,t)$ $[\gamma(p_0,t_0,t)]$ and we have set $\mu_0=1$ (by an appropriate orientation of the Cartesian axis). Since we assume that the electrons lose their energy continuously, a one-to-one relation can be established between time t and energy γ. The use of the energy rather than time is not a drawback. On the contrary, as we address the issue of the energy deposition as a function of position, γ is the pertinent variable to express range, straggling, and radius. Using $d\gamma/dt=-\gamma/p$ and Eq. (20), we obtain the inverse of the energy-loss rate per unit length,

$$\frac{d\langle z\rangle}{d\gamma} = -\frac{p^2}{\gamma^2}\left\{\frac{(\gamma-1)(\gamma_0+1)}{(\gamma+1)(\gamma_0-1)}\right\}^{(Z\Lambda+1)/2}. \tag{21}$$

Finally, an integration over the energy from γ_0 to γ with the initial condition $\langle z\rangle(\gamma_0,\gamma_0)=0$ gives us the average distance traveled along $\mathbf{e}_z$ as a function of the energy,

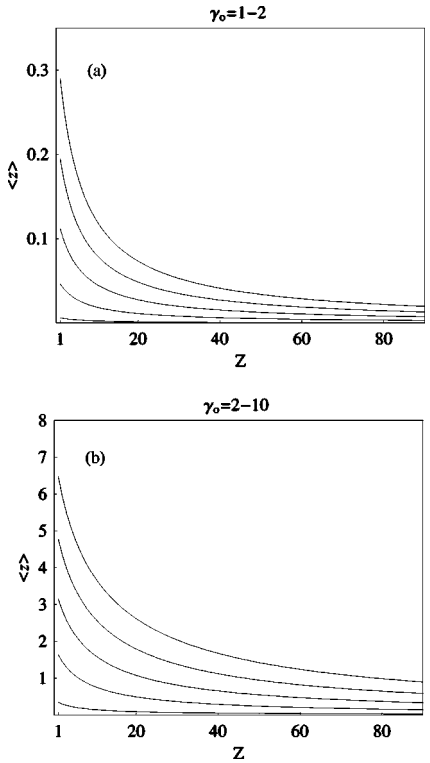

FIG. 8. Slowing down length vs ion charge Z. (a) For $\gamma_0=1.2$, 1.4, 1.6, 1.8, and 2; the upper curve is for $\gamma_0=2$. (b) For $\gamma_0=2$, 4, 6, 8, and 10; the upper curve is for $\gamma_0=10$.

$$\langle z\rangle(\gamma,\gamma_0) = \left(\frac{\gamma_0+1}{\gamma_0-1}\right)^{(Z\Lambda+1)/2}\int_{\gamma}^{\gamma_0} d\gamma\frac{p^2}{\gamma^2}\left(\frac{\gamma-1}{\gamma+1}\right)^{(Z\Lambda+1)/2}. \tag{22}$$

Equation (22) expresses the average distance traveled by a relativistic electron interacting with a plasma with ion charge state Z as a function of its initial energy γ_0.

The average full slowing down length, i.e., the *stopping length*, is obtained by setting in Eq. (22) the energy γ to rest energy $\gamma=1$, when the electron stops. For small values of Z, we can explicitly express this stopping length. For example, assuming $\Lambda=1$ and a hydrogenlike target $Z=1$, we obtain from Eq. (22)

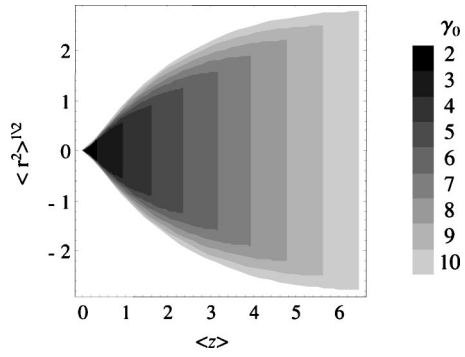

FIG. 9. Energy deposition in a hydrogenlike plasma ($Z=1$) for electron energy ranging from $\gamma_0=2$ to $\gamma_0=10$.

$$\langle z\rangle(1;\gamma_0)=\frac{\gamma_0+1}{\gamma_0-1}\left(\gamma_0-\frac{1}{\gamma_0}-2\ln\gamma_0\right). \tag{23}$$

For example, the explicit expression for $Z=3$ is reported in the final section.

In Fig. 4, we have plotted the energy γ as a function of the traveled length for an initial energy equal to 1 MeV ($\gamma_0=2$) for $Z=1$ and 2; in order to illustrate the impact of the pitch angle scattering, we have also plotted the very same expression when pitch angle scattering is ignored [$Z\Lambda+1$ is set to 0 in Eq. (22)]. Clearly, pitch angle scattering shortens this slowing down length by a factor of the order 2. For $Z=1$, half of the initial energy is deposited in the plasma on the last two-fifths of the stopping length. Consider a plasma with $Z=1$ and $n=10^{32}$ cm^{-3} for which the unit length $\lambda=20$ μm. From the formula (23) applied to a 1 MeV electron, electron energy deposition ends up after 7 μm and after 10 μm when pitch angle scattering is neglected. Even for the case $Z=1$, ignoring pitch angle scattering gives rise to a large deviation from the full relativistic kinetic model. Obviously this deviation will increase with Z so that the standard slowing down model becomes particularly inappropriate for the high Z target.

Plotted in Fig. 5 is the normalized electron penetration depth $\langle z\rangle(1;\gamma_0)$ as a function of initial energy γ_0 for five low values of $Z\Lambda=1,3/2,2,5/2$, and 3; the initial kinetic energy γ_0-1 ranges from 0 MeV to 2.5 MeV. Finally, in Fig. 6, we have displayed this normalized penetration depth for various values of the charge state and initial energy; this parametric study clearly displays that the mean penetration depth tends to be a linear function of the initial energy γ_0 at an energy threshold function of the charge state. This asymptotic behavior is due to the ultrarelativistic limit $p\sim\gamma$ in Eq. (22) and to the smoothing effect of the high Z exponent in Eq. (22).

B. Straggling effect

The inclusion of pitch angle scattering also has a dramatic effect on the dispersion of the penetration depth, namely the straggling effect [22]. Many electrons will have the mean range although some will have a higher range and some will have less than this average. This results in a finite width to the electron range distribution known as *range straggling*. To define this range straggling s, we introduce the root-mean-square deviation around the average longitudinal range,

$$s(\gamma,\gamma_0)=\sqrt{\langle z^2\rangle(\gamma,\gamma_0)-\langle z\rangle^2(\gamma,\gamma_0)}. \tag{24}$$

In the previous section, we have already calculated $\langle z\rangle$ so that in order to calculate s, we have now to evaluate $\langle z^2\rangle$. This latter quantity is related to the *velocity autocorrelation function*. We first note that

$$\frac{d\langle z^2\rangle}{dt}=\left\langle\frac{dz^2}{dt}\right\rangle=2\left\langle z(t)\frac{dz(t)}{dt}\right\rangle. \tag{25}$$

Then, for a given realization of the stochastic variable $\mu=\cos\theta$, the electron trajectory is a Brownian path whose projection on $\mathbf{e}_z$ is the (random) distance $z(t)$,

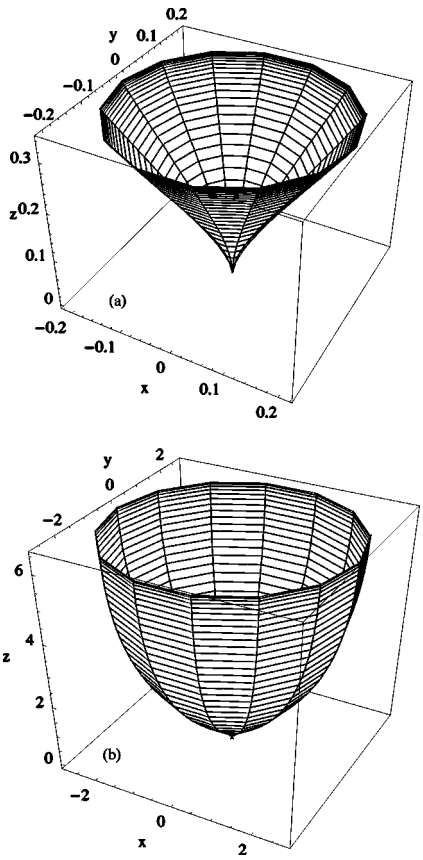

FIG. 10. Energy deposition in a hydrogenlike plasma ($Z=1$) for electron initial energy equal to $\gamma_0=2$ (a) and $\gamma_0=10$ (b).

$$z(t)=\int_0^t dt'\frac{dz}{dt'}(t')=\int_0^t dt' v_z(t'). \tag{26}$$

Substituting Eq. (26) into Eq. (25) and commuting integration and averaging bracket yields

$$\frac{d\langle z^2\rangle}{dt}=2\int_0^t dt'\langle v_z(t)v_z(t')\rangle. \tag{27}$$

To express $\langle z^2\rangle$, we integrate Eq. (27) with respect to time in order to obtain

$$\langle z^2\rangle(t,t_0)=2\int_0^t dt'\int_0^{t'} dt''\langle v_z(t'')v_z(t')\rangle. \tag{28}$$

The quantity $\Gamma_{zz}(t'',t')=\langle v_z(t'')v_z(t')\rangle$ is the *two time longitudinal velocity autocorrelation function* and can be calculated with the Green function of the collision operator. Note that in Γ_{zz}, we have $t\geqslant t'\geqslant t''$.

An electron starting at time $t_0=0$ with the momentum $\mathbf{p}_0$ will be found with the probability $G(\mathbf{p}',\mathbf{p}_0,t',t_0)d\mathbf{p}$ at later time t' in the momentum volume element $d\mathbf{p}'$ centered around $\mathbf{p}'$. Then, this very same electron will be found at time t'' with momentum $\mathbf{p}''$ with the probability $G(\mathbf{p}'',\mathbf{p}',t'',t')d\mathbf{p}''$ in the momentum volume element $d\mathbf{p}''$ around $\mathbf{p}''$. Hence, the conditional probability (density) to

find this electron at time t' with momentum $\mathbf{p}'$ and at time t'' with momentum $\mathbf{p}''$ is the product $P(\mathbf{p}'',\mathbf{p}',\mathbf{p}_0,t'',t',t_0)$ of these two probabilities,

$$P(\mathbf{p}'',\mathbf{p}',\mathbf{p}_0,t'',t',t_0)d\mathbf{p}'d\mathbf{p}'' = G(\mathbf{p}'',\mathbf{p}',t'',t')G(\mathbf{p}',\mathbf{p}_0,t',t_0)d\mathbf{p}'d\mathbf{p}''. \quad (29)$$

Note that if we integrate this later formula over the intermediate momentum $\mathbf{p}'$, we just recover the Chapman-Kolmogorov identity Eq. (11). The two-time longitudinal velocity autocorrelation function $\Gamma_{zz}(t',t'')$ is the average over all the realization of the product $v_z(t'')v_z(t')$ over this probability P,

$$\Gamma_{zz}(t',t) = \int\int d\mathbf{p}\; d\mathbf{p}' P(\mathbf{p}',\mathbf{p},\mathbf{p}_0,t',t,t_0)\frac{pp'}{\gamma\gamma'}\cos\,\theta\cos\,\theta'. \quad (30)$$

After some lengthy calculations, reported in the Appendix, involving Clebsch-Gordan calculus, we end up with an explicit formula for $\langle z^2\rangle$,

$$\langle z^2\rangle(\gamma;\gamma_0) = \frac{2}{3}\int_{\gamma_0}^{\gamma} d\gamma' \frac{\gamma'^2-1}{\gamma'^2}\left(\frac{\gamma'-1}{\gamma'+1}\right)^{(Z\Lambda+1)/2}\int_{\gamma_0}^{\gamma'} d\gamma'' \frac{\gamma''^2-1}{\gamma''^2}\left(\frac{\gamma''+1}{\gamma''-1}\right)^{(Z\Lambda+1)/2} + 2\left(\frac{\gamma_0+1}{\gamma_0-1}\right)^{[3(Z\Lambda+1)]/2}\int_{\gamma_0}^{\gamma'} d\gamma' \frac{\gamma''^2-1}{\gamma''^2}\left(\frac{\gamma''-1}{\gamma''+1}\right)^{Z\Lambda+1}. \quad (31)$$

These integrals can be evaluated for integer values of $Z\Lambda+1/2$; despite the fact that the standard symbolic calculator provides an analytical closed form of these integral, the final result contains a fairly large number of terms so that we report here only the $Z=1$ case corresponding to a hydrogenlike plasma,

$$\langle z^2\rangle(1;\gamma_0) = \{-9-9\gamma_0+171\gamma_0^2+16\pi^2\gamma_0^2-213\gamma_0^3+48\pi^2\gamma_0^3+213\gamma_0^4+48\pi^2\gamma_0^4-171\gamma_0^5+16\pi^2\gamma_0^5+9\gamma_0^6+9\gamma_0^7 + 192\mathrm{Li}_2(2,-\gamma_0)\gamma_0^2(1+\gamma_0)^3-24\gamma_0^2\ln\,\gamma_0(3+15\gamma_0+9\gamma_0^2+5\gamma_0^3)-12\gamma_0(1+\gamma_0)\ln\,\gamma_0[3-6\gamma_0-2\gamma_0^2-6\gamma_0^3 + 3\gamma_0^4-16\gamma_0(1+\gamma_0)^2\ln(1+\gamma_0)]\}/[9\gamma_0^2(\gamma_0-1)^3], \quad (32)$$

where Li_2 is the dilogarithm function [23].

In Fig. 7, we have plotted $s(1;\gamma_0)$ as a function of the initial energy for $Z=1$ and 2. For low initial energy, below 2 MeV, s is of order of $\langle z\rangle/2$. This means that the energy deposition volume (hot spot) extended over a distance of the order of the stopping length, i.e., the hot spot is broad. However, for higher energy above 2 MeV [Fig. 7(b)], $\langle z\rangle$ increases faster than s and the energy deposition localization is better defined than at low energy.

VI. MEAN-SQUARE RADIUS

As a result of multiple small-angle Coulomb scattering off background plasma, a fast electron beam expands radially during its propagation. This radial expansion determines the size of the energy deposition volume. While this effect is supposed to be important only for relatively high Z, we will show that it has, in fact, a dramatic impact even for a hydrogen plasma.

To quantify this radial spreading, we define the mean square radius $\langle r^2\rangle$,

$$\frac{d\langle r^2\rangle}{dt} = \left\langle \frac{d(x^2+y^2)}{dt}\right\rangle = 4\left\langle x(t)\frac{dx}{dt}\right\rangle. \quad (33)$$

Along the very same steps used to derive Eq. (28) from Eq. (25), we can relate this mean-square radius to the *two-time transverse velocity autocorrelation function* $\Gamma_{xx}=\langle v_x(t'')v_x(t')\rangle$,

$$\langle r^2\rangle(t,t_0) = 4\int_0^t dt'\int_0^{t'} dt''\langle v_x(t'')v_x(t')\rangle, \quad (34)$$

where Γ_{xx} is given by

$$\Gamma_{xx} = \int\int d\mathbf{p}\; d\mathbf{p}' P(\mathbf{p}',\mathbf{p},\mathbf{p}_0,t',t,t_0)\frac{pp'}{\gamma\gamma'} \times\sin\,\theta\sin\,\theta'\cos\,\phi\cos\,\phi'. \quad (35)$$

The explicit calculation of $\langle r^2\rangle$, reported in the Appendix, leads to the final result

$$\langle r^2\rangle(\gamma;\gamma_0) = \frac{4}{3}\int_{\gamma}^{\gamma_0} d\gamma' \frac{\gamma'^2-1}{\gamma'^2}\left(\frac{\gamma'-1}{\gamma'+1}\right)^{(Z\Lambda+1)/2}\int_{\gamma'}^{\gamma_0} d\gamma'' \frac{\gamma''^2-1}{\gamma''^2}\left(\frac{\gamma''+1}{\gamma''-1}\right)^{(Z\Lambda+1)/2} - \left(\frac{\gamma_0+1}{\gamma_0-1}\right)^{[3(Z\Lambda+1)]/2}\int_{\gamma'}^{\gamma_0} d\gamma'' \frac{\gamma''^2-1}{\gamma''^2}\left(\frac{\gamma''-1}{\gamma''+1}\right)^{Z\Lambda+1}. \tag{36}$$

Note that Eq. (36) differs from Eq. (31) only by a numerical factor inside the integral over γ''. The $Z=1$ and $Z=2$ cases are displayed in Fig. 7; it confirms the expected dramatic impact of pitch angle scattering for $Z=1$ and 2: $\langle r^2\rangle \sim \langle z\rangle^2$. For the sake of completeness, we report below the analytical result for $Z=1$,

$$\langle r^2\rangle(1;\gamma_0) = -\frac{4}{9}\{9-45\gamma_0+4\pi^2\gamma_0+138\gamma_0^2+12\pi^2\gamma_0^2-138\gamma_0^3+12\pi^2\gamma_0^3+45\gamma_0^4+4\pi^2\gamma_0^4-9\gamma_0^5+48\gamma_0\,\mathrm{Li}_2(-\gamma_0)(1+\gamma_0)^3 - 12\gamma_0\ln\gamma_0(3+3\gamma_0+9\gamma_0^2+\gamma_0^3)+6\gamma_0(1+\gamma_0)\ln\gamma_0[-3+10\gamma_0-3\gamma_0^2+8(1+\gamma_0)^2\ln(1+\gamma_0)]\}/[\gamma_0^2(\gamma_0-1)^3]; \tag{37}$$

when Z is an integer, $\langle r^2\rangle$ can also be expressed analytically [23].

VII. DISCUSSION AND CONCLUSION

In this paper, we have addressed the problem of the characteristic size of the energy deposition volume for relativistic electrons interacting with a cold plasma. The hot spot where most of the energy is deposited is characterized by three lengths: the stopping length, the straggling length, and the mean-square transverse radius. In order to calculate these three lengths, we have solved the relativistic kinetic equation which extends the *Landau* collisional operator to the relativistic regime. The method proposed here, based on the Green function of this relativistic operator, turned out to be very efficient; for example, we were able to express these three lengths. Equation (22), which is one of the three main results of this paper, gives the range of a relativistic electron in a Lorentzian plasma. Our method is not restricted to the $Z=1$ hydrogenlike case. As a matter of fact, for $Z=3$ the stopping length is simply given by

$$\left[\frac{\langle z\rangle(1;\gamma_0)}{\mathrm{cm}}\right] = \left(\frac{\gamma_0+1}{\gamma_0-1}\right)^2\left(4\ln\frac{4\gamma_0}{(1+\gamma_0)^2}+\frac{1-\gamma_0^2}{\gamma_0^2}\right) \times \frac{1}{\ln\Lambda_{ee}}\left[\frac{10^{30}\ \mathrm{m}^{-3}}{n_e}\right]. \tag{38}$$

Moreover, the two other results Eqs. (31) and (36) provide the two other characteristic lengths of the hot spot.

This set of formulas allows us to study the parametric dependence of the hot spot size. The impact of Z is in fact important, as illustrated in Fig. 8, where the behavior of the stopping length as a function of the charge state is depicted. In Fig. 9, we have plotted $\langle r^2\rangle$ as a function of $\langle z\rangle$ for several initial energies in order to visualize the heated volume. A 3D plot of the very same curves is depicted in Fig. 10 and provides a representation of the shape and size of the heated volume for initial energy equal to 1 MeV and 5 MeV.

Besides this problem of the hot spot characteristic sizes, our Green-function formalism is well suited to address a certain number of other important issues. The impact of beam self-generated electric and magnetic field can be explored through a perturbative expansion based on the field-free Green function G. A criterion for self-pinching can be established. The calculation of bremsstrahlung emission by relativistic electrons relies on an accurate description of the energy and the pitch angle dynamic; again the Green function G is the right tool to provide this description. All of these topics will be considered in further studies.

APPENDIX: CALCULATION OF THE VELOCITY AUTOCORRELATION FUNCTION

1. The longitudinal autocorrelation function

We report here in this appendix the calculation of the longitudinal velocity autocorrelation function $\Gamma_{zz} = \langle v_z(t'')v_z(t')\rangle$. We first express the velocity v_z and v_x with the spherical momentum coordinates

$$v_z = \frac{p}{\gamma}\cos\theta, \quad v_x = \frac{p}{\gamma}\sin\theta\cos\varphi. \tag{A1}$$

Then, using the identities

$$\cos\theta = \sqrt{\frac{4\pi}{3}}Y_1^0(\theta,\varphi),$$

$$\sin\theta = \sqrt{\frac{2\pi}{3}}[Y_1^1(\theta,\varphi)-Y_{-1}^1(\theta,\varphi)], \tag{A2}$$

we write down the component of the velocity in terms of spherical harmonic functions

$$v_z = \sqrt{\frac{4\pi}{3}}\frac{p}{\gamma}Y_1^0(\theta,\varphi),$$

$$v_x = \sqrt{\frac{2\pi}{3}}\frac{p}{\gamma}[Y_1^1(\theta,\varphi) - Y_{-1}^1(\theta,\varphi)]. \tag{A3}$$

As discussed in Sec. V B, the longitudinal velocity autocorrelation function is given by

$$\Gamma_{zz}(t,t') = \frac{4\pi}{3}\int\int d\mathbf{p}\; d\mathbf{p}' G(\mathbf{p},\mathbf{p}',t,t') \times G(\mathbf{p}',\mathbf{p}_0,t',t_0)\frac{pp'}{\gamma\gamma'}Y_1^0(\theta,\varphi)Y_1^0(\theta',\varphi'). \tag{A4}$$

In Eq. (A4), the volume element is defined as $d\mathbf{p} = p^2 dp\; d^2\Omega$. We consider first the angular integration over $d^2\Omega$ and $d^2\Omega'$. Substituting Eq. (10) for both Green functions into Eq. (A4), we obtain the following expression for the angular part of the integral in Eq. (A4),

$$\frac{4\pi}{3}\sum_{l=0}^{+\infty}\sum_{m=-l}^{m=+l}\sum_{l'=0}^{+\infty}\sum_{m'=-l'}^{m'=+l'}\int d^2\Omega\int d^2\Omega' Y_l^m(\theta,\varphi)Y_l^{m*}(\theta',\varphi')Y_{l'}^{m'}(\theta',\varphi')Y_{l'}^{m'*}(\theta_0,\varphi_0)Y_1^0(\theta,\phi)Y_1^0(\theta',\phi') \times\left\{\frac{(\gamma-1)(\gamma'+1)}{(\gamma+1)(\gamma'-1)}\right\}^{[l(l+1)(Z+1)]/4}\left\{\frac{(\gamma'-1)(\gamma_0+1)}{(\gamma'+1)(\gamma_0-1)}\right\}^{[l'(l'+1)(Z+1)]/4}. \tag{A5}$$

The integration over the solid angle $d^2\Omega$ can be performed using orthogonality properties of the spherical harmonics,

$$\int d^2\Omega Y_l^m(\theta,\varphi)Y_{l'}^{m'}(\theta,\varphi) = \delta_{ll'}\delta_{mm'}, \tag{A6}$$

whose application to Eq. (A5) yields

$$\Gamma_{zz}(t,t') = \frac{4\pi}{3}\sum_{l'=0}^{+\infty}Y_{l'}^{m'*}(\theta_0,\varphi_0)\left\{\frac{(\gamma-1)(\gamma'+1)}{(\gamma+1)(\gamma'-1)}\right\}^{(Z+1)/2}\left\{\frac{(\gamma'-1)(\gamma_0+1)}{(\gamma'+1)(\gamma_0-1)}\right\}^{[l'(l'+1)(Z+1)]/4} \times\int d^2\Omega' Y_1^{0*}(\theta',\varphi')Y_{l'}^{m'}(\theta',\varphi')Y_1^0(\theta',\varphi'). \tag{A7}$$

In Eq. (A7), we have to integrate the product of three spherical harmonic functions. For clarity, we introduce the following notation:

$$\langle Y_{l_1}^{m_1}Y_{l_2}^{m_2}Y_{l_3}^{m_3}\rangle = \frac{4\pi}{3}Y_{l_2}^{m_2}(\theta_0,\varphi_0) \times\int d^2\Omega\; Y_{l_1}^{m_1*}(\theta,\varphi)Y_{l_2}^{m_2}(\theta,\varphi)Y_{l_3}^{m_3}(\theta,\varphi); \tag{A8}$$

such quantities appearing in Eq. (A7) describe the correlation of the pitch angle at different time and include the initial pitch angle θ_0. From the theory of angular momentum addition, the integral of the product of three spherical harmonics is proportional to the Clebsch-Gordan coefficients and vanishes unless the following *selection rules* are satisfied [21]: (i) $|l_1-l_3|\leqslant l_2\leqslant l_1+l_3$, (ii) $l_1+l_2+l_3$ is an even number, and (iii) $m_2+m_3=m_1$. Thus, in Eq. (A7), we have only two coefficient $\langle Y_1^0Y_0^0Y_1^0\rangle$ and $\langle Y_1^0Y_2^0Y_1^0\rangle$ to calculate. With the use of a Clebsch-Gordan calculator, we end up with

$$\langle Y_1^0Y_0^0Y_1^0\rangle = \frac{1}{3}, \quad \langle Y_1^0Y_2^0Y_1^0\rangle = \frac{1}{3}(3\cos^2\theta_0 - 1). \tag{A9}$$

After performing the integration over the solid angle, we have to integrate over p and p' in Eq. (A4). To achieve this task, we take advantage of the following identity:

$$\delta(f(x)) = \sum_i \frac{\delta(x-x_i)}{|f'(x)|_{x=x_i}}, \tag{A10}$$

where the x_i's are the zero of the function f. This allows us to reduce the δ function in the Green function to the form

$$\delta[\arctan p - p - \arctan p_0 + p_0 - (t - t_0)] = \frac{\gamma^2(t)}{p^2(t)}\delta(p - p(p_0, t_0, t)), \tag{A11}$$

where $p(t, p_0, t_0)$ is the solution of the equation

$$\arctan p - p - \arctan p_0 + p_0 - (t - t_0) = 0. \tag{A12}$$

Using this relation, integration over p and p' is straightforward and the longitudinal correlation function is finally given by

$$\Gamma_{zz}(t,t') = \frac{1}{3}\frac{p(t)p(t')}{\gamma(t)\gamma(t')}\left[\left(\frac{[\gamma(t)-1][\gamma(t')+1]}{[\gamma(t)+1][\gamma(t')-1]}\right)^{(Z+1)/2} + (3\cos^2\theta_0 - 1)\left(\frac{\gamma(t)-1}{\gamma(t)+1}\right)^{(Z+1)/2}\left(\frac{\gamma(t')-1}{\gamma(t')+1}\right)^{Z+1}\left(\frac{\gamma_0+1}{\gamma_0-1}\right)^{[3(Z+1)]/2}\right]. \tag{A13}$$

We note, as expected, that this autocorrelation function depends on the initial pitch angle θ_0. In the main part of the paper, we consider a well-collimated beam and we can orientate the system of the axis such that $\theta_0 = 0$. In this case, the numerical factor in the square brackets reduces to 2. To calculate $\langle z^2 \rangle$, we insert Eq. (A13) into Eq. (28) and consider the change of variable $t \to \gamma$. Again, using Eq. (A11) we recover the expression Eq. (31).

2. The transverse autocorrelation function

The transverse autocorrelation function is calculated in a very similar way. In order to avoid lengthy calculations, we just report the final result here,

$$\Gamma_{xx}(t,t') = \frac{1}{3}\frac{p(t)p(t')}{\gamma(t)\gamma(t')}\left[\left(\frac{[\gamma(t)-1][\gamma(t')+1]}{[\gamma(t)+1][\gamma(t')-1]}\right)^{(Z+1)/2} - \frac{3\cos^2\theta_0 - 1}{2}\left(\frac{\gamma(t)-1}{\gamma(t)+1}\right)^{(Z+1)/2}\left(\frac{\gamma(t')-1}{\gamma(t')+1}\right)^{Z+1}\left(\frac{\gamma_0-1}{\gamma_0+1}\right)^{[3(Z+1)]/2}\right]. \tag{A14}$$

This allows us to recover Eq. (36) when $\cos\theta_0 = 1$.

[1] L. V. Spencer, Phys. Rev. **98**, 1597 (1955).
[2] L. V. Spencer, *Energy Dissipation by Fast Electrons* (National Bureau of Standards, Washington, D.C., 1959).
[3] E. Nardi and Z. Zinamon, Phys. Rev. A **18**, 1246 (1978).
[4] V. Val'chuk *et al.*, Plasma Phys. Rep. **21**, 159 (1995).
[5] W. T. Scott, Rev. Mod. Phys. **35**, 231 (1963).
[6] M. Tabak *et al.*, Phys. Plasmas **1**, 1626 (1994).
[7] J. M. Rax, J. Robiche, and I. Kostyukov, Phys. Plasmas **7**, 1026 (2000).
[8] J. M. Rax and N. J. Fisch, Phys. Rev. Lett. **69**, 772 (1992).
[9] J. M. Rax and N. J. Fisch, Phys. Fluids B **5**, 2578 (1993).
[10] G. Shvets, N. J. Fisch, and J. M. Rax, Phys. Rev. E **65**, 046403 (2002).
[11] H. W. Koch and J. W. Motz, Rev. Mod. Phys. **31**, 920 (1959).
[12] N. J. Fisch, Rev. Mod. Phys. **59**, 175 (1987).
[13] J. M. Rax, J. Robiche, and I. Kostyukov, Phys. Plasmas **6**, 3233 (1999).
[14] M. N. Rosenbluth, W. M. MacDonald, and D. L. Judd, Phys. Rev. **107**, 1 (1957).
[15] L. Landau and E. Lifshitz, *Physical Kinetics* (Pergamon Press, New York, 1981).
[16] B. A. Trubnikov, *Reviews of Plasma Physics* (Consultant Bureau, New York, 1965), Vol. 1, pp. 105–204.
[17] S. T. Belaiev and G. I. Budker, Dokl. Akad. Nauk SSSR **107**, 807 (1956).
[18] B. J. Braams and C. F. F. Karney, Phys. Rev. Lett. **59**, 1817 (1987).
[19] D. Mosher, Phys. Fluids **18**, 846 (1975).
[20] J. M. Rax, Phys. Fluids **31**, 1111 (1988).
[21] E. U. Condon and G. H. Shortley, *The Theory of Atomic Spectra* (Cambridge University Press, Cambridge, 1987).
[22] U. Fano, Annu. Rev. Nucl. Sci. 13 (1963).
[23] S. Wolfram, *The Mathematica® Book* (Cambridge University Press, Cambridge, 1996).